

## Exploring the Mechanism for the Synthesis of Silsesquioxanes. 3. The Effect of Substituents and Water

Takako Kudo\*

Department of Fundamental Studies, Faculty of Engineering, Gunma University, Kiryu 376-8515, Japan

Mark S. Gordon\*

Department of Chemistry, Iowa State University, Ames, Iowa 50011-2030

Received: June 12, 2002

The effect of various substituents on the hydrolysis and condensation reactions, the initial stages of the mechanism to form silsesquioxanes, are investigated with *ab initio* electronic structure theory including electron correlation effects. In addition, the role of water molecules on the mechanism is also discussed.

### Introduction

For many years, polyhedral oligomeric silsesquioxanes (POSS) have attracted considerable experimental and theoretical interest because of their wide variety of practical uses.<sup>1,2</sup> However, most previous studies have focused on the structures and properties of POSS compounds, or on modeling surface reactions of silica or zeolites. The mechanism(s) for the synthesis of POSS have largely been unexplored. Polysilsesquioxanes can be captured as one of the forms of silicone resins,<sup>1c</sup> for which the process (chemistry)–structure–properties relationship is not well understood. It is therefore very important to understand what molecular and electronic structural features are responsible for which property, and which reaction mechanism results in what structure for obtaining materials with new or desired properties. Although hydrolytic polycondensation of alkoxy-silanes has been extensively studied,<sup>3</sup> that for trichlorosilanes, which has been preferred in the silicon industry, is much less well studied due to their much faster reaction rates.

We have therefore initiated an *ab initio* molecular orbital study of the mechanism for the synthesis of POSS. Previous papers have presented results on the early stages of the reaction<sup>4</sup> (hydrolysis and initial condensation) as well as the further condensation to form cyclosiloxanes.<sup>5</sup> However, all compounds examined to date are the parent hydrogen silsesquioxanes, R = H in (RSiO<sub>1.5</sub>)<sub>n</sub> or (R(OH)SiO)<sub>n</sub>, even though many experimental studies have been carried with a variety of substituents. The effect of substituents is clearly expected to be an important factor in determining the reaction mechanism(s). Solvent effects are also expected to have an impact on the manner in which the reactions proceed. Indeed, previous studies have demonstrated that even one water molecule can have a significant impact on the reaction mechanisms.<sup>4,5</sup>

The current work explores the effects of both substituents and solvent (i.e., water) on the mechanisms for the synthesis of silsesquioxanes.

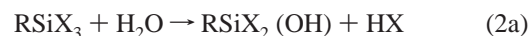
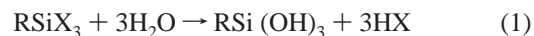
### Computational Methods

The geometries of all molecules of interest have been fully optimized at the restricted Hartree–Fock (RHF) level of theory using the 6-31G(d) basis set.<sup>6</sup> In addition, the geometries of smaller and some key systems were refined using second-order perturbation theory (MP2)<sup>7</sup> and the 6-31G(d) basis set. All

compounds were characterized as minima or transition states by calculating and diagonalizing the Hessian matrix of energy second derivatives at the HF/6-31G(d) level of theory. Single point MP2<sup>8</sup> energy calculations have been performed to obtain more reliable energetics. A small number of solvent waters have been included by employing two “supermolecule” approaches. The one or two water molecules that are in closest proximity to the *ab initio* solutes and catalyze one or more steps in the reaction were included at the same *ab initio* levels of theory as the solute molecules. Two additional spectator waters that stabilize the reaction system through hydrogen bonding were represented by the effective fragment potential (EFP) method.<sup>9</sup> All calculations were performed with the GAMESS electronic structure code.<sup>10</sup>

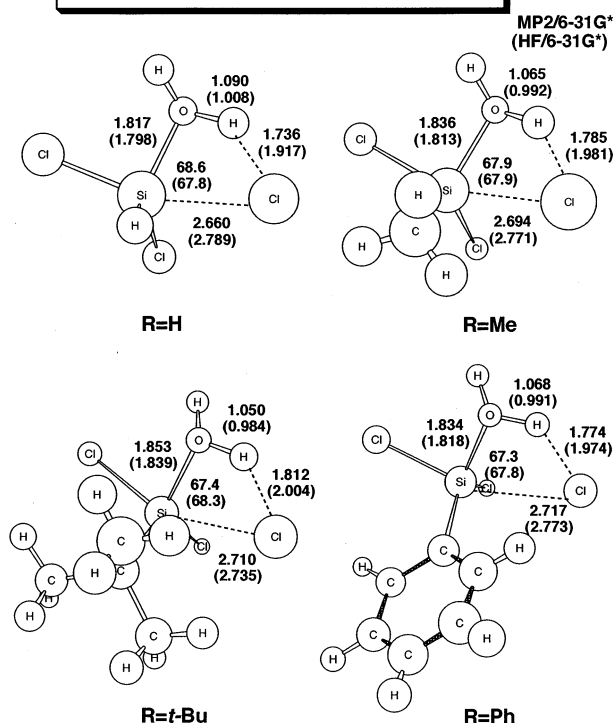
### Result and Discussion

**A. Hydrolysis.** The hydrolysis (eq 1) of a trihalosilane (RSiX<sub>3</sub>) to form trihydroxysilane (RSi(OH)<sub>3</sub>) is considered to be the first step of the synthesis of silsesquioxanes.



A previous paper in this series<sup>4</sup> demonstrated that these reactions take place in the stepwise manner illustrated by eqs 2a–c. The energy barrier for the first step (2a) was predicted to be the highest and higher than the barriers for subsequent condensation steps,<sup>5</sup> so that reaction 2a is the rate-determining step. It is therefore sensible to consider substituent effects on this first step.

Figure 1 shows the transition state structures for the first step of the hydrolysis of RSiCl<sub>3</sub> (R = H, Me, *t*-Bu, and Ph) at both the HF and MP2 levels of theory, using the 6-31G(d) basis set. Because MP2 is more reliable, the following discussion focuses on the distances predicted at this level of theory, although the HF trends are similar. As the substituent R becomes bulkier (H

TS for the hydrolysis of  $\text{RSiCl}_3$ : 1st step

**Figure 1.** Transition structures for the first step in the hydrolysis of  $\text{RSiCl}_3$  ( $R = \text{H, Me, } t\text{-Bu, and Ph}$ ) in angstroms and degrees.

**TABLE 1: MP2/6-31G(d) Substituent Effects on the First  $\text{RSiX}_3$  Hydrolysis Step (See Eq 2a in the Text)**

R	X	energy barrier (kcal/mol)	
		direct	+ $\text{H}_2\text{O}^a$
H	Cl	23.0	-1.2
Me	Cl	23.6	1.7
<i>t</i> -Bu	Cl	24.9	7.2
Ph	Cl	24.4	3.0
H	OMe	17.0	-2.7

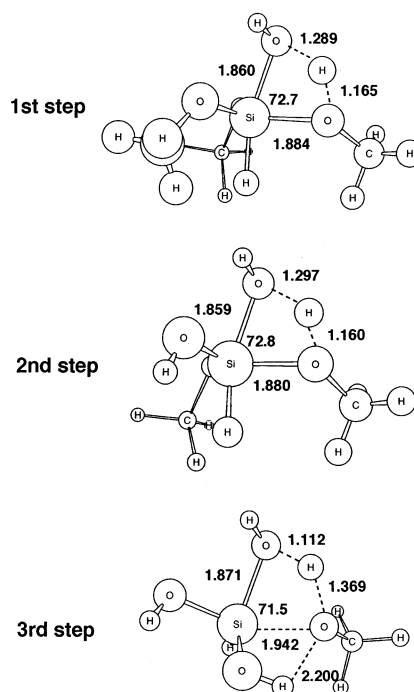
<sup>a</sup> The values are for the water-catalyzed cases.

**TABLE 2: Comparison of MP2/6-31G(d) Hydrolysis Barrier Heights for  $\text{HSiCl}_3$  vs  $\text{HSi(OMe)}_3$**

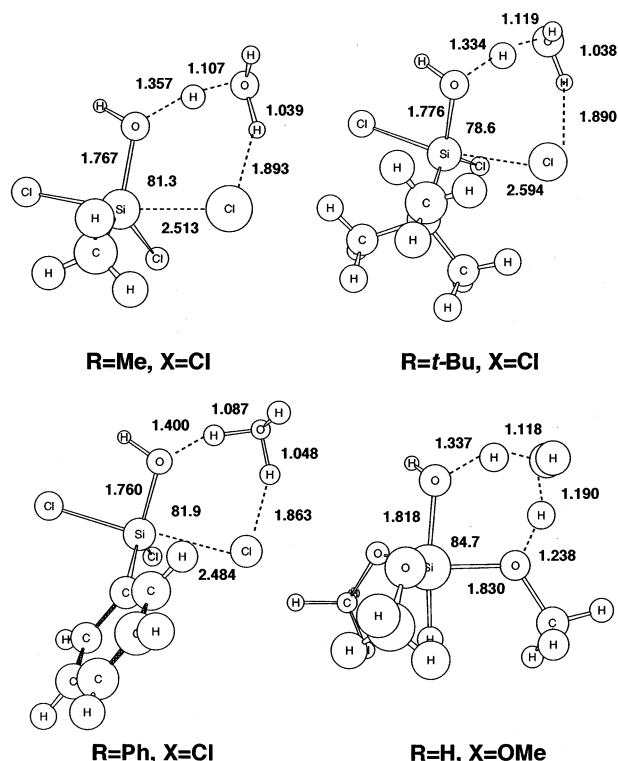
R	X	energy barrier (kcal/mol)
First Step: $\text{RSiX}_3 + \text{H}_2\text{O} \rightarrow \text{RSiX}_2(\text{OH}) + \text{HX}$		
H	Cl	23.0
H	OMe	17.0
Second Step $\text{RSiX}_2(\text{OH}) + \text{H}_2\text{O} \rightarrow \text{RSiX}(\text{OH})_2 + \text{HX}$		
H	Cl	14.7
H	OMe	16.2
Third Step $\text{RSiX}(\text{OH})_2 + \text{H}_2\text{O} \rightarrow \text{RSi}(\text{OH})_3 + \text{HX}$		
H	Cl	12.3
H	OMe	17.3

$\langle \text{Me} \sim \text{Ph} < t\text{-Bu} \rangle$ , the six-center transition state region expands: The Si-Cl, H...Cl, and Si-O distances all increase relative to  $R = \text{H}$ , probably because of the steric congestion around the Si atom.

The energy barriers for the first hydrolysis step for  $\text{RSiX}_3$  as a function of R and X are collected in Table 1. In the absence of solvent, the bulkier substituents R cause only a small increase ( $\sim 1.5\text{--}2$  kcal/mol) in the barrier. Replacing  $X = \text{Cl}$  by  $X = \text{OMe}$  decreases the barrier by  $\sim 6$  kcal/mol at the correlated levels of theory. The results in Table 1 suggest that the “gas phase” substituent effects are small, except for the predicted large decrease in barrier height for  $X = \text{OMe}$ .

MP2/6-31G\* TS for the hydrolysis of  $\text{HSi(OMe)}_3$ 

**Figure 2.** Transition structures for the three steps in the hydrolysis of  $\text{HSi(OMe)}_3$  in angstroms and degrees.

MP2/6-31G\* TS for the hydrolysis of  $\text{RSiX}_3$  catalyzed by a water: step 1

**Figure 3.** Transition structures for the first step in the hydrolysis of  $\text{RSiX}_3$  ( $R = \text{H, Me, } t\text{-Bu, and Ph}$ ;  $X = \text{Cl and OMe}$ ) with a water catalyst in angstroms and degrees.

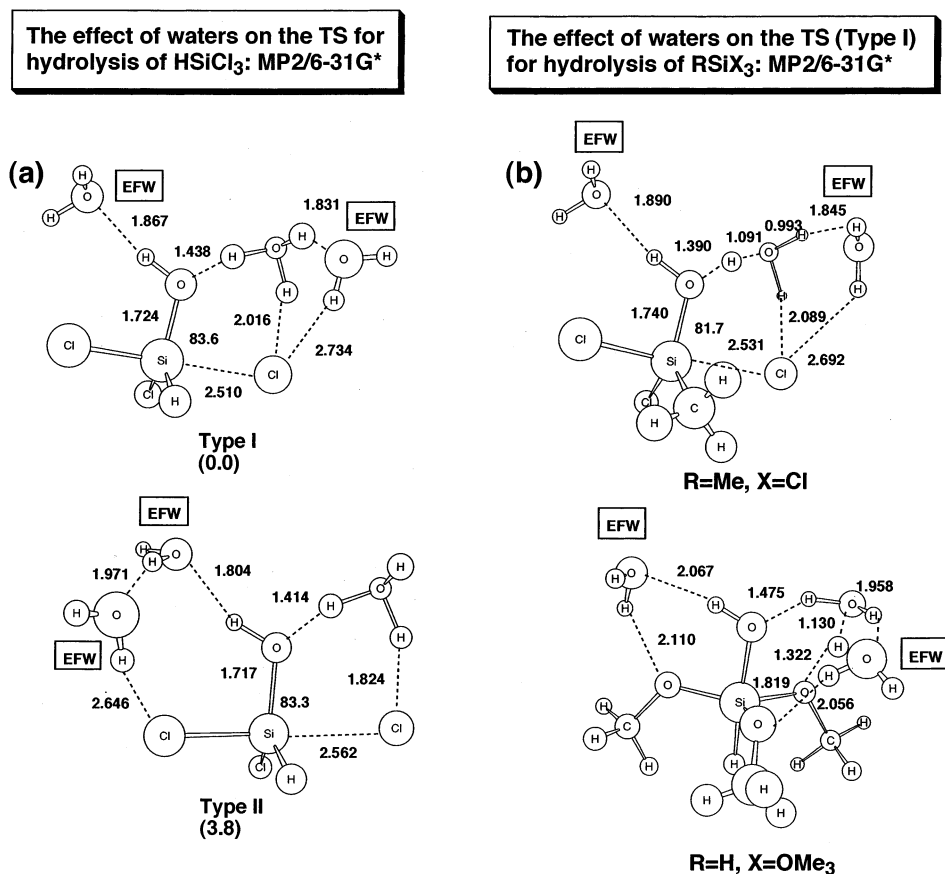


**Figure 4.** (a) Two types of transition structures for the first step in the hydrolysis of HSiCl<sub>3</sub> with a water catalyst and two effective fragment waters (labeled EFW) in angstroms and degrees. (b) Type I transition structures for the first step in the hydrolysis of MeSiCl<sub>3</sub> and HSi(OMe)<sub>3</sub> with a water catalyst and two effective fragment waters (labeled EFW) in angstroms and degrees.

To examine the effect of the methoxy group in more detail, the transition structures for all three hydrolysis steps were located and compared with the corresponding structures and energy barriers for the parent Cl compound (see Figure 2 and Table 2). For X = Cl, the energy barrier decreases monotonically from step 1 to step 3. In contrast, for X = OMe, the correlated levels of theory predict essentially no change in the barrier from step to step. It was suggested previously that intramolecular hydrogen bonding stabilizes the transition state in the second and third steps when X = Cl.<sup>4</sup> This does not appear to be the case for X = OMe, as shown in Table 2 and Figure 2.

In the previous papers,<sup>4,5</sup> it was noted that the presence of just one water molecule can have a dramatic effect on the mechanism of POSS formation. That is, the water reduces the barrier heights for the hydrolysis, initial condensation, and further condensation to form tri- and tetracyclosiloxane from large values (10–30 kcal/mol) to small or nonexistent values. Table 1 lists the water-catalyzed barrier heights as a function of substituent. The geometries are displayed in Figure 3. The OSiCl bond angle increases by 13–14° and six-centered structures are formed with an extra water in all cases. This stabilizes the transition state and lowers the barrier relative to that in the absence of water. In addition, with the water molecule present, the H is transferred to the leaving group (Cl or OMe) via the water. So, the water catalyses the H transfers. As shown previously, the effect on the energy barrier is dramatic: The barriers are all reduced by up to 20 kcal/mol. In addition, the presence of the water molecule has a quantitatively different effect depending on the substituent. There is little steric substituent effect for X = Cl in the gas phase, with a range of less than 2 kcal/mol. When the water is added, the barrier for

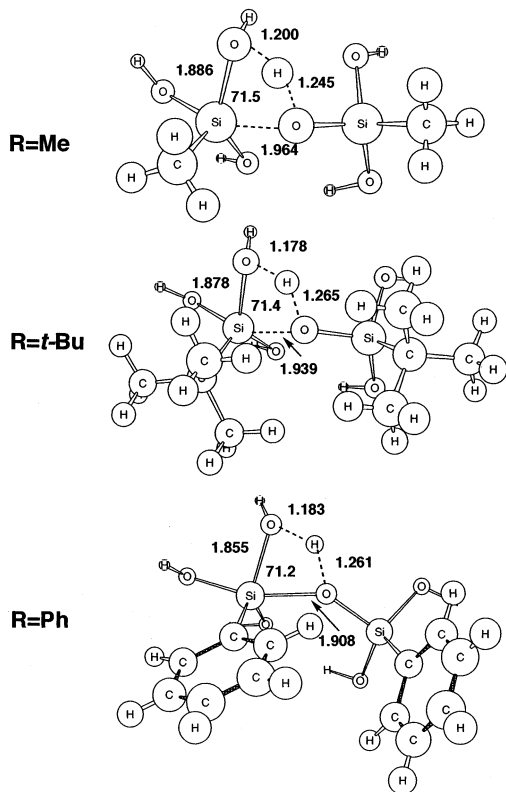
R = *t*-Bu is considerably larger than that for R = H, even though the additional water does decrease the gas phase barrier by 17 kcal/mol. Substituting R = OMe for R = Cl has little effect on the water-assisted barrier height.

Of course, in an actual reaction with excess water, there exist additional water molecules, which do not participate directly in the hydrolysis reaction but rather stabilize the system through hydrogen bonding. Therefore, consider the effect on the first step hydrolysis transition state of two additional water molecules that are represented using the EFP method. Two alternative orientations of the two waters are considered: In type I the two EFP waters are not directly interacting. In type II the two waters are connected by a hydrogen bond. Figure 4a shows the two kinds of transition structures for the first step of the HSiCl<sub>3</sub> hydrolysis, with one catalyst water and two EFP waters (denoted as EFW in the figure). In both type I and type II structures, the Si...Cl distance is longer than the corresponding distance (2.457 Å) in the transition structure without the effective fragment waters. This suggests a later transition state when the EFP waters are present. The leaving Cl atom in type I forms a hydrogen bond with the *ab initio* water and apparently a weak interaction with one EFW. In type II, the leaving Cl interacts only with the *ab initio* water. Type I is found to be more stable than type II by 3.8 kcal/mol at the MP2/6-31G(d) level of theory.<sup>11</sup> As Table 3 shows, when the two EFP waters are added in a type I arrangement, the energy barrier for the hydrolysis decreases significantly relative to the case with just one catalyst water, for both R = H and R = Me. As shown in Table 3, the effective fragment waters also significantly decrease the barrier for both X = Cl and X = OMe. Figure 4b shows the type I transition structures for R = Me, X = Cl, and R = H, X = OMe.

**TABLE 3: MP2/6-31G(d) Effect of Waters on the First Step of  $\text{RSiX}_3$  Hydrolysis**

R	X	energy barrier (kcal/mol)		
		direct	+ H <sub>2</sub> O	+ 2EFW <sup>a</sup>
$\text{RSiX}_3 + \text{H}_2\text{O} \rightarrow \text{RSiX}_2(\text{OH}) + \text{HX}$				
H	Cl	23.0	-1.2	-17.2
Me	Cl	23.6	1.7	-13.8
H	OMe	17.0	-2.7	-21.8

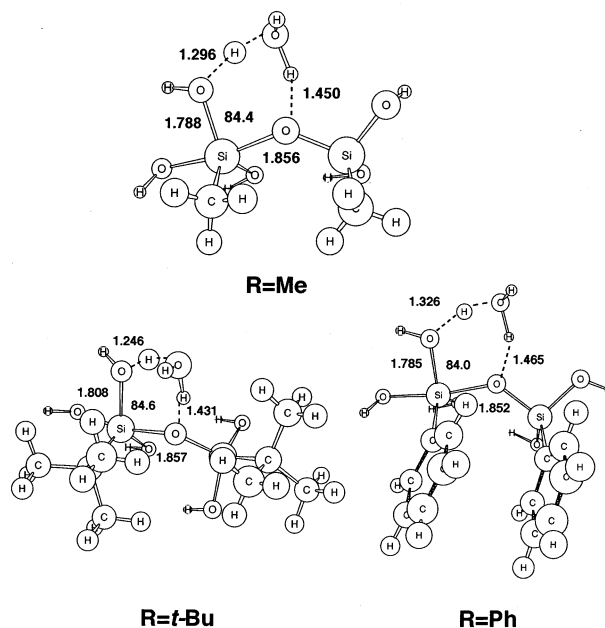
<sup>a</sup> Waters treated by effective fragment potential method, type I structure in Figure 4.

**TS for the condensation of  $\text{RSi}(\text{OH})_3$  : MP2/6-31G\*****Figure 5.** Transition structures for the condensation of  $\text{RSi}(\text{OH})_3$  (R = Me, *t*-Bu, and Ph) in angstroms and degrees.

**B. Initial Condensation: Formation of Dimer.** Next consider the condensation reaction,



for R = H, Me, *t*-Bu, Ph. First, consider the effect of substituents. The transition structures for the direct reaction and the water-catalyzed reaction are displayed in Figures 5 and 6, respectively. Note that the central Si - - O distance for the newly forming Si-O bond is not elongated as R becomes bulkier (see Figure 5). In fact, for the *t*-Bu species, this Si - - O distance (1.939 Å) is shorter than that in the Me analogue. This trend is continued in the Ph compound. As a result, the four-centered transition structure is somewhat compressed with bulkier substituents. The OSiO bond angle, consisting of the newly forming Si-O bond and the Si-O(H) bond, is similar for the three compounds. For the water-catalyzed reaction (Figure 6), the central Si - - O distance is essentially the same for all three substituents. So, the steric effect of the bulky substituent may be slightly

**TS for the condensation of  $\text{RSi}(\text{OH})_3$  catalyzed by a water : MP2/6-31G\*****Figure 6.** Transition structures for the condensation of  $\text{RSi}(\text{OH})_3$  (R = Me, *t*-Bu, and Ph) with a catalyzed water in angstroms and degrees.**TABLE 4: MP2/6-31G(d) Substituent Effects on the Initial Condensation Barrier for  $\text{RSi}(\text{OH})_3$  (See Eq 3 in Text)**

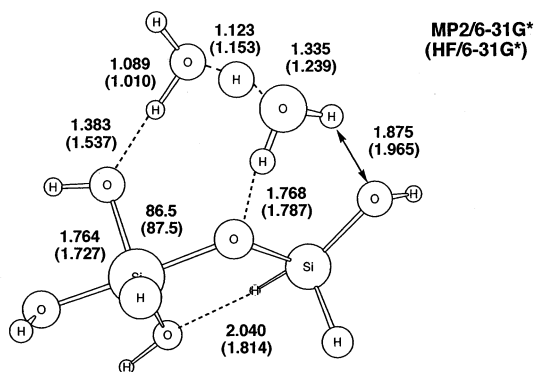
R	energy barrier (kcal/mol)	
	direct	+ H <sub>2</sub> O <sup>a</sup>
H	10.9	-9.3
Me	7.7	-13.3
<i>t</i> -Bu	9.8	-9.3
Ph	7.9	-16.4

<sup>a</sup> The values are for the water-catalyzed reactions.

more important in this case than in the direct reaction. It is also interesting that for R = *t*-Bu, the Si(OH) group distorts its position to avoid steric interaction with the adjacent Me groups.

Table 4 presents the calculated barrier heights for the condensation reaction (3). In the gas phase, all substituents lower the condensation barrier slightly, by 1–3 kcal/mol, relative to the unsubstituted parent  $\text{HSi}(\text{OH})_3$ . As noted for the hydrolysis reactions, the addition of one (catalyst) water causes the condensation barriers to disappear for all substituents. This means that the transition structures of all species are significantly stabilized by the newly formed hydrogen bonds with an additional water relative to the reactants. As for the parent  $\text{HSi}(\text{OH})_3$  in the previous study,<sup>4</sup> the negative barriers occur because there are low-energy hydrogen-bonded intermediate complexes in the entrance channel. No attempt was made to find these intermediates for the substituted species in the present study. In contrast to the hydrolysis, it seems that the steric effect is not important for the initial condensation reaction.

For the condensation reaction, it is interesting to examine the effect of a second *ab initio* water on the reaction barrier. Can a second water participate directly in the condensation and thereby further stabilize the transition state? As Figure 7 shows, two hydrogens transfer via an eight-centered transition structure, and they each move almost on a straight line between two oxygens. The hydrogen bonding indicated by the arrow in the figure plays an important role in stabilizing the second water.

Condensation of HSi(OH)<sub>3</sub> with two extra waters

transition structure

## Energy Barriers (kcal/mol)

	direct	+ H <sub>2</sub> O	+ 2H <sub>2</sub> O
HF/6-31G*	30.4	16.7	0.8
MP2/6-31G*	10.9	-9.3	-31.4

Figure 7. Transition structure for the condensation of HSi(OH)<sub>3</sub> with two catalyzed waters in angstroms and degrees.

In the hydrolysis reaction, this kind of structure has not been found, possibly because the additional (Si)OH group is not present. As indicated in the figure, the second water causes as large a decrease in the barrier height as does the first water.

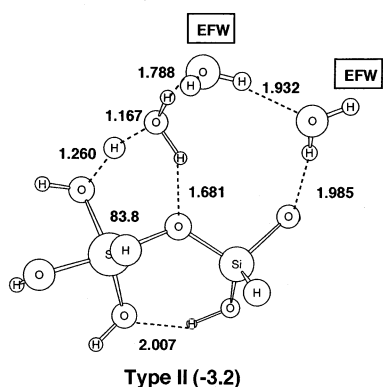
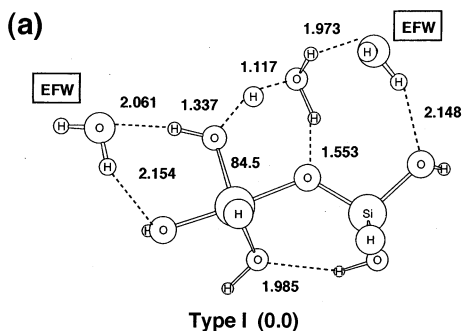
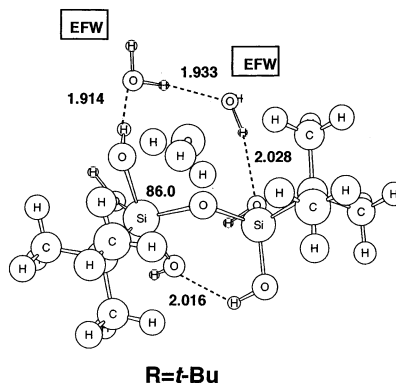
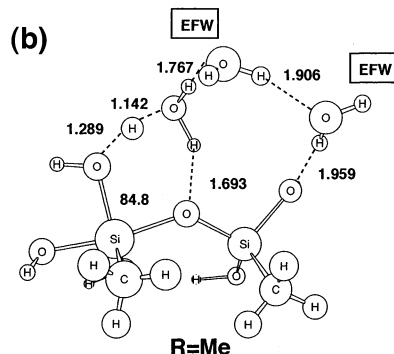
The effect of waters on the TS for the condensation of HSi(OH)<sub>3</sub>: MP2/6-31G\*The effect of waters on the TS (Type II) for the condensation of RSi(OH)<sub>3</sub>: MP2/6-31G\*

Figure 8. (a) Two types of transition structures for the condensation of HSi(OH)<sub>3</sub> with a catalyzed water and two effective fragment waters (labeled as EFW) in angstroms and degrees. (b) Type II transition structures for the condensation of MeSi(OH)<sub>3</sub> and *t*-BuSi(OH)<sub>3</sub> with a water catalyst and two effective fragment waters (labeled EFW) in angstroms and degrees.

TABLE 5: Effect of Waters on the Initial MP2/6-31G(d) RSi(OH)<sub>3</sub> Condensation Barrier

R	energy barrier (kcal/mol)		
	direct	+ H <sub>2</sub> O	+ 2EFW <sup>a</sup>
RSi(OH) <sub>3</sub> + RSi(OH) <sub>3</sub> → R(OH) <sub>2</sub> SiOSi(OH) <sub>2</sub> R + H <sub>2</sub> O			
H	10.9	-9.3	-33.9
Me	7.7	-13.3	-28.4
<i>t</i> -Bu	9.8	-9.3	-22.2

<sup>a</sup> Waters treated by effective fragment potential method.

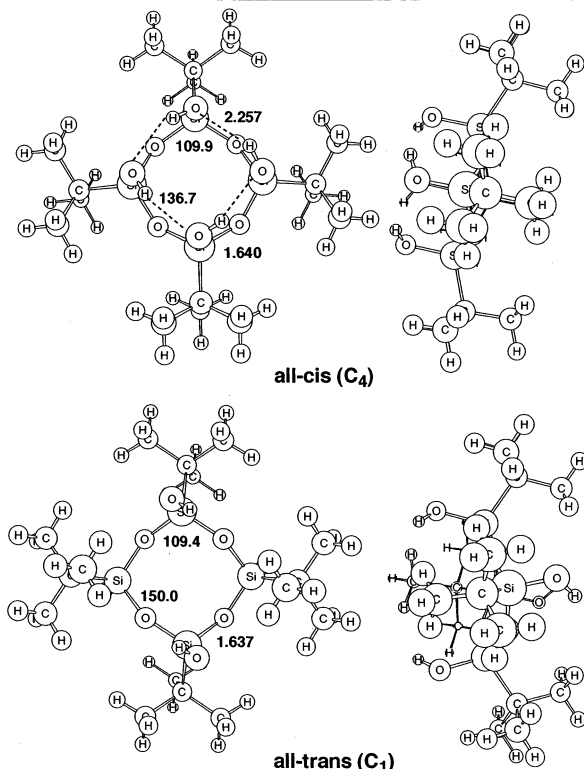
As illustrated in Figure 8a, the addition of two EFP waters results in two types of transition structure for the HSi(OH)<sub>3</sub> condensation, analogous to those found for the hydrolysis reaction. In contrast to the hydrolysis reaction, the type I arrangement is less stable than type II by 3.2 kcal/mol. The OH group attached to the Si on the right appears to provide some stabilization via hydrogen bonding. The analogous type II structures for the Me and *t*-Bu species are displayed in Figure 8b as well. For the *t*-Bu compound, the orientation of the two EFP waters is different from that of the H or Me analogues, even though the optimization was initiated using the orientation obtained from the smaller substituents. Despite considerable effort, it was not possible to locate the analogous transition structure for R = Ph. This may mean that this TS does not exist.<sup>12</sup> The corresponding energy barriers are summarized in Table 5. For all compounds, the energy barrier is dramatically reduced by the addition of two EFWs compared with only one ab initio water. The effect of the waters surrounding the reacting molecules is therefore predicted to be significant.

**C. Ring Formation (Condensation).** Next consider the effects of substitution on the structures and formation energetics

**TABLE 6: Some HF/6-31G(d) Geometric Parameters<sup>a</sup> (Ångstroms and Degrees) for [R(OH)SiO]<sub>n</sub> (R = H, Me, and *t*-Bu; *n* = 3 and 4)**

R	<i>r</i> (SiO)	∠OSiO	∠SiOSi	∠SiOSiO	∠CSiO <sup>b</sup>
D <sub>3</sub>					
H(C <sub>1</sub> ) <sup>c</sup>	1.641	106.1	132.9	11.9	109.1
Me(C <sub>3</sub> )	1.646	106.4	131.3	21.7	111.2
<i>t</i> -Bu(C <sub>3</sub> )	1.649	106.3	128.7	31.5	111.6
D <sub>4</sub>					
H(C <sub>4</sub> )	1.636	110.6	136.5	74.4	112.7
Me(C <sub>4</sub> )	1.640	110.0	136.6	75.0	112.9
<i>t</i> -Bu(C <sub>4</sub> )	1.641	109.9	136.7	75.3	112.7

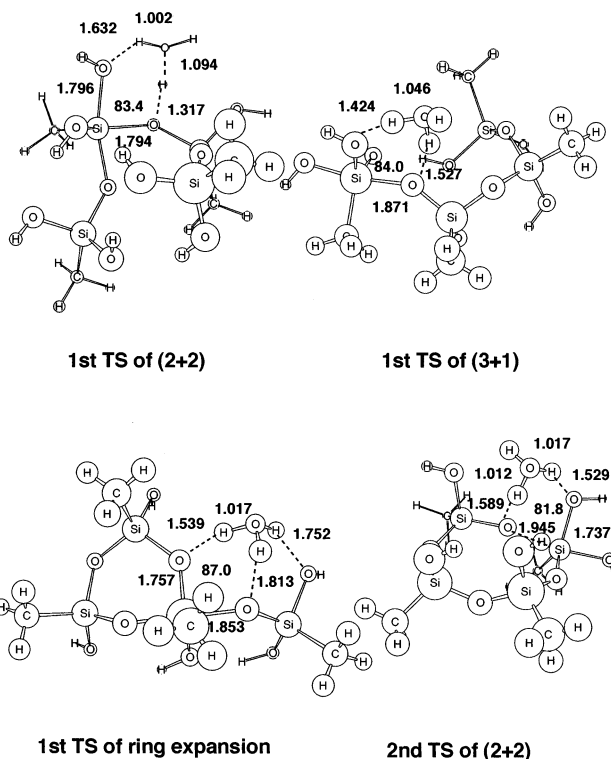
<sup>a</sup> Averaged values. <sup>b</sup> Bond angle between the α carbon of R and oxygen of the OH group attached to silicon atoms. <sup>c</sup> Molecular symmetry.

**Two isomers of D<sub>4</sub> (OH, *t*-Bu): HF/6-31G\***

**Figure 9.** HF/6-31G\* optimized structure of two isomers of tetrahydroxytetra-*tert*-butylcyclotetrasiloxane, (R(OH)SiO)<sub>4</sub>; R = *t*-Bu, in angstroms and degrees. Top views are on the left side, and side views are on the right side.

for cyclotrisiloxanes (D<sub>3</sub>) and cyclotetrasiloxanes (D<sub>4</sub>). The substituent effects on the geometries of D<sub>3</sub> and D<sub>4</sub> are summarized in Table 6. The values quoted in the table are averaged geometric parameters for the all-cis isomer with all OH groups “above” the ring. This arrangement was found to be the most stable for both D<sub>3</sub> and D<sub>4</sub>.<sup>4</sup> The D<sub>4</sub> eight-membered ring seems to be more folded (nonplanar) than D<sub>3</sub>, on the basis of the larger SiOSiO dihedral angles (~75.0°). However, the other parameters are very similar in the six- (D<sub>3</sub>) and eight-membered (D<sub>4</sub>) rings. The substituent effects on the geometry are more significant in D<sub>3</sub> than in D<sub>4</sub>. For D<sub>3</sub>, as the substituent becomes bulkier, the SiOSiO dihedral angle increases, and the SiOSi bond angle decreases. For D<sub>4</sub>, in contrast, all parameters are almost unchanged upon the substitution of bulky groups.

Next, consider the effect of substituents on the relative stability of the ring isomers. For the parent hydrogen compound, it was found that the all-cis isomer is the most stable for D<sub>3</sub>

**TSS for the formation of methyl substituted D<sub>4</sub> with an extra water: HF/6-31G\***

**Figure 10.** Transition structures for methyl substituted D<sub>4</sub> in the presence of the water catalyst in angstroms and degrees.

and D<sub>4</sub> because of the hydrogen bonding among the OH groups. The least stable isomer is the all-trans structure, in which the OH groups are arranged alternatively above and below the ring.<sup>5</sup> This is in agreement with the experimental evidence for D<sub>4</sub> with R = *i*-Pr.<sup>13</sup> The MP2/6-31G(d)//HF/6-31G(d) energy (in kcal/mol) of the all-cis isomer of substituted D<sub>4</sub> (R(OH)SiO)<sub>4</sub> relative to the all-trans isomer is -9.8 (R = H), -10.4 (R = Me), and -11.3 (R = *t*-Bu), respectively. So, for all species, the all-cis isomer is more stable than the all-trans and the stability increases with the bulkiness of the substituent.

Figure 9 shows the two isomers of the *t*-Bu species. In the all-cis isomer, four OH groups are in the center of the ring facilitating effective hydrogen bonding, whereas the *t*-Bu groups are arranged outside of the ring to minimize steric effects between neighboring groups. In the all-trans form, on the other hand, the *tert*-butyl groups are more congested. As seen in the figure, the resulting strain causes the all-trans ring to twist, and the SiOSi bond angle increases to 150.0°.

Now, consider the effect of methyl substitution on the formation of D<sub>4</sub>. As in the parent compound,<sup>5</sup> we have considered three kinds of stepwise reaction mechanisms for the methyl substituted D<sub>4</sub> formation: (1) 2+2 condensation, (2) 3+1 condensation, and (3) ring expansion from D<sub>3</sub>. The four transition structures for the water-catalyzed condensation are displayed in Figure 10. As in the previous study, it is assumed that the ring-closure step is the same in all mechanisms. The geometric character is almost unchanged upon methyl substitution.

The corresponding energetics are collected in Table 7. As reported in the previous study,<sup>4</sup> all these reactions have two steps. For the first (2+2) mechanism, both energy barriers are higher for the methyl compound than for the H compound. However, methyl substitution has essentially no effect on the

**TABLE 7: Effect of Methyl Group on the MP2/6-31G(d)//HF/6-31G(d) D<sub>4</sub> Formation<sup>a</sup>**

	TS1	TS2	products
	I. (2+2)		
H	9.9 (-14.0) <sup>b</sup>	18.6 (-4.9)	-8.7
Me	12.9 (-10.1)	21.5 (2.3)	-8.4
	II. (3+1)		
H	9.9 (-17.3)	21.1 (-2.4)	-8.8
Me	9.7 (-14.2)	21.1 (1.9)	-8.9
	III. Ring Expansion		
H	13.0 (-12.7)	8.5 (-15.0)	-18.7
Me	11.5 (-11.6)	7.5 (-11.6)	-22.4

<sup>a</sup> Energies (kcal/mol) relative to the reactants. <sup>b</sup> The values in parentheses are for the water-catalyzed cases.

barriers in the second (3+1) mechanism. The barriers for the third (ring expansion) mechanism actually decrease slightly upon methyl substitution.<sup>14</sup> For the water-catalyzed mechanisms, all barriers are small or zero for both R = H and R = Me. In summary, the effect of a methyl group on D<sub>4</sub> formation is small, and there is a large solvent effect.

### Concluding Remarks

The effects of substituents and a limited number of waters on the hydrolysis, initial condensation (for dimer formation) and further condensation to form cyclosiloxanes, have been investigated in the present study. For the hydrolysis of RSiCl<sub>3</sub>, the energy barrier in the gas phase reaction decreases in the order, R = *t*-Bu ~ Ph > Me > H. This trend is the same in the presence of an additional water molecule acting as a catalyst, but the energy differences are larger than those in the gas phase reaction. The effect of replacing the -Cl leaving groups with methoxy groups in the initial hydrolysis step was also investigated. It is found that HSi(OMe)<sub>3</sub> has the smallest energy barrier among all species.

Because the synthesis of POSS compounds is performed in solution, most commonly in aqueous solution, the effect of additional (solvent) waters was examined using the effective fragment potential (EFP) method, for RSiCl<sub>3</sub> (R = H and Me) and HSi(OMe)<sub>3</sub>. The effect of adding these solvent molecules is to greatly reduce the energy barriers in the first hydrolysis, leaving no net barrier.

Somewhat surprisingly, in contrast to the initial, hydrolysis step, for the initial condensation to form the siloxane R<sub>3</sub>Si-O-SiR<sub>3</sub>, the substitutions R = Me, *t*-Bu, and Ph are found to have smaller energy barriers than that predicted for the parent hydrogen compound in the gas phase reaction. This suggests that the potential steric effect of the *t*-Bu group does not play a significant role on this reaction. For the water-catalyzed reaction, the condensation of all compounds proceeds without a barrier, in analogy with the hydrolysis reaction. The same disappearance of the condensation barriers is observed when two effective fragment solvent molecules are added to the system for R = H, Me, and *t*-Bu species.

The second condensation (ring formation) reaction to form cyclotetrasiloxanes (D<sub>4</sub>) has three possible two-step mechanisms. The effect of methyl substitution and a water catalyst was investigated for these three alternative mechanisms. In analogy with the earlier steps in the mechanism, the catalyst water reduces the barrier to zero, or nearly zero, in all three mechanisms. The preference for the all-cis isomer relative to the all-trans isomer in D<sub>4</sub> apparently increases as the bulkiness of the substituent increases. The effect of methyl substitution on D<sub>4</sub> formation is predicted to be small.

**Acknowledgment.** We are grateful to Drs. Gregg Zank and Maki Itoh for informative discussions. This work has been supported by a Grant-in-Aid on Priority-Area Research: Material Design and Reaction Control by Molecular Physical Chemistry (11166212), Dow Corning Asia Ltd. (T.K.), and the Air Force Office of Scientific Research (M.S.G.). Computer time has been made available via a Grand Challenge grant from the DOD High Performance Computing Modernization Office on the T3E computers at ERDC and AHPARC and a grant from the Computer Center of the Institute for Molecular Science.

### References and Notes

- (1) As the reviews, for example: (a) Voronkov, M. G.; Lavrent'yev, V. L. *Top. Curr. Chem.* **1982**, *102*, 199. (b) Feher, F. J.; Newman, D. A.; Walzer, J. F. *J. Am. Chem. Soc.* **1989**, *1111*, 1741. (c) Baney, R. H.; Itoh, M.; Sakakibara, A.; Suzuki, T. *Chem. Rev.* **1995**, *95*, 1409. (d) Feher, F. J.; Budzichowski, T. A. *Polyhedron* **1995**, *14*, 3239.
- (2) As the recent paper, for example: (a) Duchateau, R.; Cremer, U.; Harmsen, R. J.; Mohamud, S. I.; Abbenhuis, H. C. L.; van Santen, R. A.; Meetsma, A.; Thiele, S. K. H.; van Tol, M. F. H.; Kranenburg, M. *Organometallics* **1999**, *18*, 5447. (b) Duchateau, R.; van Santen, R. A.; Yap, G. P. A. *Organometallics* **2000**, *19*, 809. (c) Abbenhuis, H. C. L. *Chem. Eur. J.* **2000**, *6*, 25. (d) Skowronska-Ptasinska, M. D.; Duchateau, R.; van Santen, R. A.; Yap, G. P. A. *Organometallics* **2001**, *20*, 3519. (e) Lorenz, V.; Spoida, M.; Fischer, A.; Edelman, F. T. *J. Organomet. Chem.* **2001**, *625*, 1. (f) Itoh, M. *Keiso Kagaku Kyokaiishi* **2001**, *15*, 19 (*Journal the Society of Silicon Chemistry Japan*). (g) Kudo, T.; Gordon, M. S. *J. Phys. Chem. A* **2001**, *105*, 11276.
- (3) (a) C. J. Brinker; G. W. Scherer *Sol-Gel Science, The Physics and Chemistry of Sol-Gel Processing*; Academic Press: San Diego, 1990. (b) Ng, L. V.; Thompson, P.; Sanchez, J.; Macosko, C. W.; McCormick, A. V. *Macromolecules* **1995**, *28*, 6471. (c) Kasehagen, L. J.; Rankin, S. E.; McCormick, A. V.; Macosko, C. W. *Macromolecules* **1997**, *30*, 3921. (d) Rankin, S. E.; Macosko, C. W.; McCormick, A. V. *Chem. Mater.* **1998**, *10*, 2037. (e) Rankin, S. E.; Kasehagen, L. J.; McCormick, A. V.; Macosko, C. W. *Macromolecules* **2000**, *33*, 7639. (f) Matejka, L.; Dukh, O.; Hlavata, D.; Meissner, B.; Brus, J. *Macromolecules* **2001**, *34*, 6904. (g) Kim, H.-J.; Lee, J.-K.; Kim, J.-B.; Park, E. S.; Park, S.-J.; Yoo, D. Y.; Yoon, D. Y. *J. Am. Chem. Soc.* **2001**, *123*, 12121.
- (4) Kudo, T.; Gordon, M. S. *J. Am. Chem. Soc.* **1998**, *120*, 11432.
- (5) Kudo, T.; Gordon, M. S. *J. Phys. Chem. A* **2000**, *104*, 4058.
- (6) (a) Hehre, W. J.; Ditchfield, R.; Pople, J. A. *J. Phys. Chem.* **1972**, *56*, 2257. (b) Francl, M. M.; Pietro, W. J.; Hehre, W. J.; Binkley, J. S.; Gordon, M. S.; Defrees, D. J.; Pople, J. A. *J. Chem. Phys.* **1982**, *77*, 3654. (c) Clark, T.; Chandrasekhar, J.; Spitznagel, G. W.; Schleyer, P. v. R. *J. Comput. Chem.* **1983**, *4*, 294. (d) Spitznagel, G. W.; Diplomarbeit, Erlangen, 1982. (e) Frisch, M. J.; Pople, J. A.; Binkley, J. S. *J. Chem. Phys.* **1984**, *80*, 3265. (f) Okuno, Y. J.; *Chem. Phys.* **1996**, *105*, 5817 and references therein.
- (7) Pople, J. A.; Seeger, R.; Krishnann, R. *Int. J. Quantum Chem.* **1979**, *S11*, 149.
- (8) Krishnann, R.; Frisch, M. J.; Pople, J. A. *J. Chem. Phys.* **1980**, *72*, 4244.
- (9) (a) Day, P. N.; Jensen, J. H.; Gordon, M. S.; Webb, S. P.; Stevens, W. J.; Krauss, M.; Garmer, D.; Basch, H.; Cohen, D. *J. Chem. Phys.* **1996**, *105*, 1968. (b) Chen, W.; Gordon, M. S. *J. Chem. Phys.* **1996**, *105*, 11081. (c) Day, P. N.; Pachter, R. *J. Chem. Phys.* **1997**, *107*, 2990. (d) Merrill, G. N.; Gordon, M. S. *J. Phys. Chem. A* **1998**, *102*, 2650. (e) Webb, S. P.; Gordon, M. S. *J. Phys. Chem. A* **1999**, *103*, 1265. (f) Petersen, C. P.; Gordon, M. S. *J. Phys. Chem. A* **1999**, *103*, 4162. (g) Gordon, M. S.; Freitag, M. A.; Bandyopadhyay, P.; Jensen, J. H.; Kairys, V.; Stevens, W. J. *J. Phys. Chem. A* **2001**, *105*, 293.
- (10) Schmidt, M. W.; Baldrige, K. K.; Boatz, J. A.; Elbert, S. T.; Gordon, M. S.; Jensen, J. H.; Koseki, S.; Matsunaga, N.; Nguyen, K. A.; Su, S.; Windus, T. L.; Dupuis, M.; Montgomery, J. A., Jr. *J. Comput. Chem.* **1993**, *14*, 1347.
- (11) In an attempt to locate lower energy arrangements of the EFP waters, Monte Carlo calculations with simulated annealing [Day, P. N.; Pachter, R.; Gordon, M. S.; Merrill, G. N. *J. Chem. Phys.* **2000**, *112*, 2063] have been performed using the HF/3-21G\* method and a temperature range from 2000–100 K. No structures lower in energy than type I were found.
- (12) The transition state was found to lie lower in energy than the reactants by 9.6 kcal/mol at the HF/6-31G\* level.
- (13) Unno, M.; Takada, K.; Matsumoto, H. *Chem. Lett.* **1998**, 489.
- (14) Note that the energy barrier for the first step decreases to 5.0 kcal/mol upon *t*-Bu substitution at the same level of theory.